International Journal of Applied Mechanics
Vol. 3, No. 2 (2011) 299–311

DOI: 10.1142/S1758825111001007

Imperial College Press
www.icpress.co.uk

CAVITATION INSTABILITY IN RUBBER

K. Y. VOLOKH

Faculty of Civil and Environmental Engineering
Technion — Israel Institute of Technology, Haifa 32000, Israel

Received 26 November 2010
Accepted 26 January 2011

Rubber materials and structures can fracture because tensile deformation and growth of small pre-existing voids become unstable, leading to failure localization and crack propagation. Thus, it is important to predict the onset of static instability of the growing voids. We consider two typical cases of interest: the instability of 3D voids under the remote hydrostatic tension in the bulk and the instability of 2D voids under the remote biaxial tension in the membrane. For the purpose of analysis, we use constitutive models of natural and styrene-butadiene rubbers with the failure description enforced by energy limiters. The limiters provide the saturation value for the strain energy which indicates the maximum energy that can be stored and dissipated by an infinitesimal material volume. We find that the unstable growth of a 3D bulk void can start when the remote hydrostatic tension reaches the value of $\sim 2 \div 3$ MPa and the unstable growth of a 2D membrane void can start when the remote biaxial tension reaches the value of $\sim 50 \div 60$ MPa.

Keywords: Rubber; cavitation; void growth; instability; elasticity; energy limiters.

1. Introduction

Unstable growth of voids or cavities is a typical mechanism of material failure. Cavitation instabilities generally occur in the material regions undergoing hydrostatic tension and they can lead to failure localization and crack propagation. Various studies have been done on modeling cavitation in elastic [Williams and Schapery, 1965; Ball, 1982; Abeyaratne and Horgan, 1985; Lopez-Pamies, 2009; Henao, 2009] and elastic-plastic [Durban and Baruch, 1976; Bassani *et al.*, 1980; Huang *et al.*, 1991; Hou and Abeyaratne, 1992] materials. Review papers by Gent [1990], Horgan and Polignone [1995], and Fond [2001] put special emphasis on cavitation in rubberlike materials. While the quoted works consider mainly 3D voids in the bulk material, a separate series of studies has been devoted to the instability of 2D voids in thin material sheets — membranes — under the biaxial tension [Durban and Birman, 1982; Haughton, 1986, 1990; Xinchun and Changjun, 2002; Cohen and Durban, 2010].

In the present work, we study the instability of a spherical bulk void under the remote hydrostatic tension (Sec. 3) and the instability of a circular membrane void

under the remote biaxial tension (Sec. 4) by using hyperelasticity with energy limiters (Sec. 2). The limiters provide the saturation value for the strain energy which indicates the maximum energy that can be stored and dissipated by an infinitesimal material volume. The main outcome of our studies are the approximate critical values, $\sim 2 \div 3\,\text{MPa}$ and $\sim 50 \div 60\,\text{MPa}$, of the remote tension, which can lead to the initiation of rubber failure in the bulk and membrane accordingly through the unstable growth of small voids.

2. Constitutive Models of Rubber Including Failure Description

In this section, we describe constitutive models of natural and styrene-butadiene rubbers that incorporate a failure description. The latter is achieved by including energy limiters in the hyperelastic strain energy functions. The basic physical idea behind the introduction of the energy limiters can be explained as follows. Let us consider an interaction of two particles, which can be molecules or molecular clusters as shown in Fig. 1. The interaction undergoes repulsion, attraction, and separation. The separation starts at the limit point of the force-distance curve shown on the right diagram of Fig. 1. The limit point appears due to the existence of the energy limiter — the bond energy — for the particle potential shown on the left diagram in Fig. 1. In the case of solids that comprise billions of particles, the average interparticle distance is measured by strain tensors and the average particle potential is measured by the strain energy function. Amazingly, in contrast to the particle interaction, the classical elasticity theory describing multi-particle systems does not include the energy limiter, which should be the average bond energy. Thus, the particle separation and consequently, material failure, is beyond the scope of the traditional elasticity theories.[1] However, the failure description can still be introduced in elasticity by analogy with the failure description in the particle interaction. The latter idea was put forward in a series of publications [Volokh, 2007, 2008, 2010].

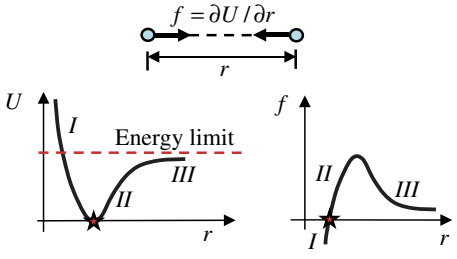

Fig. 1. Particle interaction: I–Repulsion; II–Attraction; III–Separation.

[1]Short reviews of nonlinear elasticity with examples can be found in Beatty [1987] and Ogden [2003].

A very simple yet general way to introduce the energy limiters is by using the following formula for the strain energy [Volokh, 2007]

$$\psi(\Phi, W) = \Phi \left\{ 1 - \exp\left(-\frac{W}{\Phi} \right) \right\}, \tag{1}$$

where W is the strain energy of an intact, i.e., without failure, material and Φ is the energy limiter, which can also be interpreted as the average bond energy or the failure energy. The latter provides the saturation value for the strain energy indicating the maximum energy that can be stored and dissipated by an infinitesimal material volume.

Formula (1) has two limit cases. If the failure energy is infinite, which means $\Phi \to \infty$, then we have the classical hyperelastic material: $\psi(\infty, W) = W$. If the failure energy is finite then the increase of the strain energy is limited: $\psi(\Phi, \infty) = \Phi$.

An example of the use of (1) can be found in Volokh and Vorp [2008] for the incompressible material of the Abdominal Aortic Aneurysm (AAA) with the intact strain energy in the form of $W = \alpha_1(\lambda_1^2 + \lambda_2^2 + \lambda_3^2 - 3) + \alpha_2(\lambda_1^2 + \lambda_2^2 + \lambda_3^2 - 3)^2$, $J = \lambda_1\lambda_2\lambda_3 = 1$, where λ_is are the principal stretches and material constants $\alpha_1 = 10.3\,\mathrm{N/cm^2}$; $\alpha_2 = 18.0\,\mathrm{N/cm^2}$; $\Phi = 40.2\,\mathrm{N/cm^2}$ were calibrated in the uniaxial tension test shown in Fig. 2.

We emphasize that the energy limiter is calibrated in the macroscopic failure experiments.

It is evident from Fig. 2 that formula (1) is useful for a description of smooth failure[2] with a flat limit point on the stress-strain curve, which corresponds to a gradual process of the bond rupture. However, in the case of more abrupt bond ruptures, a much sharper transition to the material instability occurs. To describe such sharp transition to failure formula (1) can be generalized as follows [Volokh, 2010]:

$$\psi = \frac{\Phi}{m} \left\{ \Gamma\left(\frac{1}{m}, 0 \right) - \Gamma\left(\frac{1}{m}, \frac{W^m}{\Phi^m} \right) \right\}. \tag{2}$$

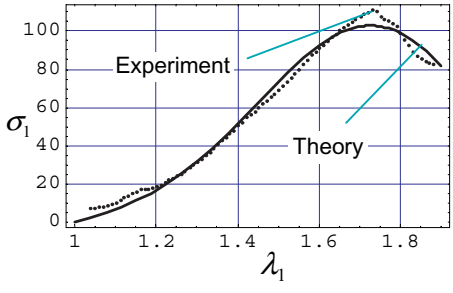

Fig. 2. Cauchy stress [N/cm^2] versus stretch in the uniaxial tension of AAA material (from Volokh and Vorp, [2008]).

[2]Other examples are reviewed in Volokh [2008].

where the upper incomplete gamma function $\Gamma(s,x) = \int_x^\infty t^{s-1}\exp(-t)\,dt$ is used.

New parameter m controls the sharpness of the transition to material instability on the stress-strain curve. Increasing or decreasing m it is possible to simulate more/less catastrophic ruptures of the internal bonds. It should not be missed that (2) reduces to (1) for $m = 1$.

Formula (2) can be applied to a filled Natural Rubber (NR) vulcanizate with the following intact strain energy calibrated by Hamdi *et al.* [2006]

$$W_{NR} = \sum_{k=1}^{3} C_{k0}(\lambda_1^2 + \lambda_2^2 + \lambda_3^2 - 3)^k, \quad J = \lambda_1\lambda_2\lambda_3 = 1, \tag{3}$$

where λ_i are principal stretches and $C_{10} = 0.298\,\text{MPa}$, $C_{20} = 0.014\,\text{MPa}$, $C_{30} = 0.00016\,\text{MPa}$.

Based on the experiments by Hamdi *et al.* [2006], who found the critical failure stretch in uniaxial tension: $\lambda_c^{NR} = 7.12$, the energy limiter $\Phi = 82.0\,\text{MPa}$ was calibrated for $m = 10$ as shown in Fig. 3 [Volokh, 2010].

Formula (2) can also be applied to a filled Styrene-Butadiene Rubber (SBR) vulcanizate with the following intact strain energy calibrated by Hamdi *et al.* [2006]:

$$W_{SBR} = \sum_{k=1}^{2} \frac{\mu_k}{\alpha_k}(\lambda_1^{\alpha_k} + \lambda_2^{\alpha_k} + \lambda_3^{\alpha_k} - 3), \quad J = \lambda_1\lambda_2\lambda_3 = 1, \tag{4}$$

where $\mu_1 = 0.638\,\text{MPa}$, $\alpha_1 = 3.03$, $\mu_2 = -0.025\,\text{MPa}$, $\alpha_2 = -2.35$.

Based on the experiments by Hamdi *et al.* [2006], who found the critical failure stretch in uniaxial tension: $\lambda_c^{SBR} = 6.88$, the energy limiter $\Phi = 94.71\,\text{MPa}$ was calibrated for $m = 10$ as shown in Fig. 4 [Volokh, 2010].

At this point we have to emphasize that elasticity with energy limiters does not include a description of the energy dissipation in its theoretical setting. Such description is irrelevant for the static problems considered in the present work because no unloading occurs. However, the account of the dissipation is crucial for modeling dynamic failure where the elastic unloading can potentially lead to the healing of

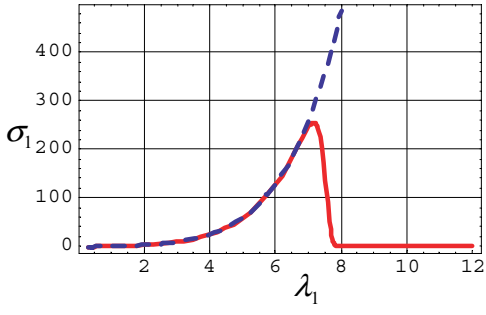

Fig. 3. Cauchy stress [MPa] versus stretch in uniaxial tension of NR: dashed line designates the intact model; solid line designates the model with energy limiter $\Phi = 82.0\,\text{MPa}$ for $m = 10$.

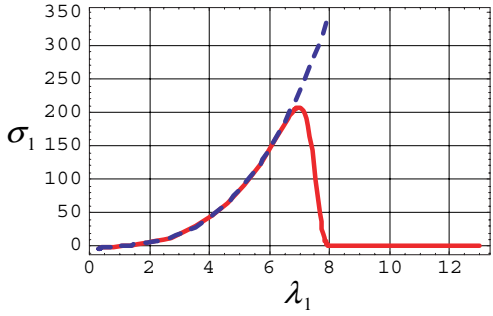

Fig. 4. Cauchy stress [MPa] versus stretch in uniaxial tension of SBR: dashed line designates the intact model; solid line designates the model with energy limiter $\Phi = 94.71$ MPa for $m = 10$.

the damaged material. To prevent the healing, the dissipation is easily enforced computationally by removing the failed finite elements from the mesh. Thus, the account of the dissipation is a technical rather than a theoretical issue (see Trapper and Volokh [2010] and Volokh [2011], for example).

3. Bulk Void

In this section, we consider the deformation of a thick-walled rubber sphere under hydrostatic tension. Assuming that the deformation is centrally-symmetric and the base vectors in spherical coordinates coincide with the principal directions of stretches, we can write the deformation law as follows

$$r = r(R), \quad \vartheta = \Theta, \quad \omega = \Omega, \tag{5}$$

where a material particle occupying position (R, Θ, Ω) in the initial configuration is moving to position (r, ϑ, ω) in the current configuration.

Designating the radial direction with Index 1 and tangential direction with Indices 2 and 3 we can write the principal stretches in the form

$$\lambda_1 = \frac{dr}{dR}, \quad \lambda_2 = \lambda_3 = \frac{r}{R}. \tag{6}$$

Since the volume of incompressible material is preserved during deformation we have

$$b^3 - a^3 = B^3 - A^3, \tag{7}$$

where A and B are the internal and a and b are the external radii of the sphere before and after deformation accordingly. We also notice that any sub-sphere with the internal or external radius $r(R)$ should also preserve its volume and, consequently, we get

$$r^3 - a^3 = R^3 - A^3. \tag{8}$$

The principal components of the Cauchy stress are in the directions of the base vectors

$$\sigma_1 = \sigma_{rr} = -p + \lambda_1 \frac{\partial \psi}{\partial \lambda_1},$$
$$\sigma_2 = \sigma_{\vartheta\vartheta} = -p + \lambda_2 \frac{\partial \psi}{\partial \lambda_2}, \tag{9}$$
$$\sigma_3 = \sigma_{\omega\omega} = -p + \lambda_3 \frac{\partial \psi}{\partial \lambda_3}$$

where p is indefinite Lagrange multiplier.

The stresses should obey the only equilibrium equation

$$\frac{d\sigma_{rr}}{dr} + 2\frac{\sigma_{rr} - \sigma_{\vartheta\vartheta}}{r} = 0. \tag{10}$$

This equation can be integrated as follows

$$\sigma_{rr}(b) - \sigma_{rr}(a) = 2\int_a^b \frac{\sigma_{\vartheta\vartheta} - \sigma_{rr}}{r} dr, \tag{11}$$

or

$$g = 2\int_a^b \left(\lambda_2 \frac{\partial \psi}{\partial \lambda_2} - \lambda_1 \frac{\partial \psi}{\partial \lambda_1}\right) \frac{dr}{r}, \tag{12}$$

where boundary conditions have been taken into account

$$\sigma_{rr}(r = a) = 0, \quad \sigma_{rr}(r = b) = g. \tag{13}$$

We notice that hydrostatic tension g is a function of the placement of the internal boundary, a, with account of

$$R(r, a) = \sqrt[3]{r^3 - a^3 + A^3}. \tag{14}$$

To make the formulation dimensionless with respect to length we rewrite (12) as follows:

$$g = 2\int_{\bar{a}}^{\bar{b}} \left(\lambda_2 \frac{\partial \psi}{\partial \lambda_2} - \lambda_1 \frac{\partial \psi}{\partial \lambda_1}\right) \frac{d\bar{r}}{\bar{r}}, \tag{15}$$

where

$$\lambda_1 = \frac{R^2}{r^2} = \frac{\bar{R}^2}{\bar{r}^2}, \quad \lambda_2 = \lambda_3 = \frac{r}{R} = \frac{\bar{r}}{\bar{R}}, \tag{16}$$

$$\bar{r} = \frac{r}{A}, \quad \bar{R} = \frac{R}{A}, \quad \bar{a} = \frac{a}{A}, \quad \bar{b} = \frac{b}{A}, \tag{17}$$

$$\bar{R}(\bar{r}, \bar{a}) = \sqrt[3]{\bar{r}^3 - \bar{a}^3 + 1}. \tag{18}$$

For $\bar{b} \gg \bar{a}$ we have the problem of the expansion of small void in the infinite medium under the remote hydrostatic tension.[3] The graph defined by (15) relates

[3]In computations we have assumed: $\bar{b} = 1000$.

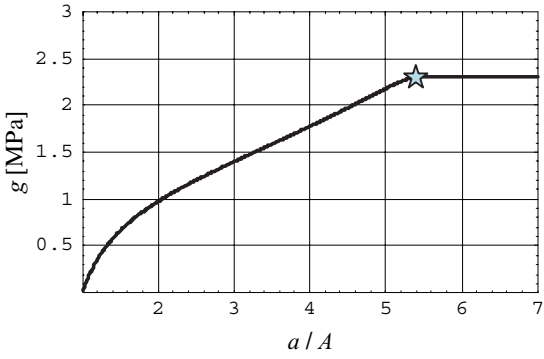

Fig. 5. 3D void: hydrostatic tension versus void hoop stretch for NR.

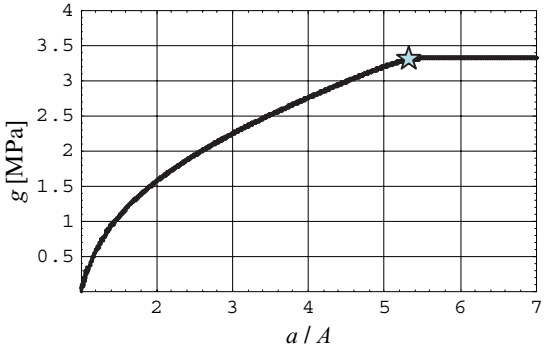

Fig. 6. 3D void: hydrostatic tension versus void hoop stretch for SBR.

the tension with the void hoop stretch, $\bar{a} = a/A$. The results of the numerical integration of (15) are presented in Figs. 5 and 6 for natural and styrene-butadiene rubbers accordingly.

The results show that starting from the hydrostatic tension of 2.3 MPa for natural rubber and 3.3 MPa for styrene-butadiene rubber the void expands unstably — it yields. Interestingly, for both materials the starred instability point corresponds to the same critical hoop stretch at the void edge: $a/A = 5.4$. It should be highlighted that the unstable yield of the void is a result of the assumption of the centrally-symmetric deformation. This assumption is restrictive, of course, and it will be violated for real materials which are not perfect. The latter will trigger localization of failure in the vicinity of the critical starred point. Nonetheless, the prediction of the critical point of the void instability seems to be reasonable even in the presence of imperfections.

Remark. It is worth emphasizing that there is no general agreement on the definition of the void instability and different authors use different definitions. In the

present work, we define the instability of the void as an event when the increase of the void size does not require further increase of the load. Such event is designated by stars on Figs. 5 and 6. The post-critical yield on the stress-stretch curves is of minor interest because it considers the highly idealized behavior of the material undergoing perfect centrally symmetric progressive failure at the void edge. It is clear, however, that material imperfections will cause non-symmetric failure modes initiating the failure localization into cracks. Thus, only the point of the onset of instability is of practical value.

4. Membrane Void

In this section, we consider the biaxial tension of a membrane rubber disk. By using cylindrical coordinates we define the referential region occupied by the membrane as follows

$$A \leq R \leq B, \quad 0 \leq \Theta \leq 2\pi, \quad -H/2 \leq Z \leq H/2. \tag{19}$$

The membrane region after the deformation is

$$a \leq r \leq b, \quad 0 \leq \vartheta \leq 2\pi, \quad -h/2 \leq z \leq h/2. \tag{20}$$

We assume that the deformation is axisymmetric and a material particle occupying position (R, Θ, Ω) in the reference configuration moves to position (r, ϑ, ω) in the current configuration in accordance with the following law

$$r = r(R), \quad \vartheta = \Theta, \quad z = \frac{h(R)}{H} Z. \tag{21}$$

Based on (21) we calculate the deformation gradient in cylindrical coordinates

$$\mathbf{F} = \begin{pmatrix} \dfrac{dr}{dR} & 0 & 0 \\ 0 & \dfrac{r}{R} & 0 \\ \dfrac{dh}{dR}\dfrac{Z}{H} & 0 & \dfrac{h}{H} \end{pmatrix}. \tag{22}$$

Since the membrane is thin, we will use the deformation gradient averaged over the thickness

$$\langle \mathbf{F} \rangle = \begin{pmatrix} \dfrac{dr}{dR} & 0 & 0 \\ 0 & \dfrac{r}{R} & 0 \\ 0 & 0 & \dfrac{h}{H} \end{pmatrix}, \tag{23}$$

where the average is defined as follows

$$\langle \mathbf{F} \rangle = \frac{1}{H} \int_{-H/2}^{H/2} \mathbf{F} dZ. \tag{24}$$

We notice that the transition from (22) to (23) brings a great simplification since the directions of the base vectors in cylindrical coordinates coincide with the average principal stretches. Based on (23) and designating the radial, tangential, and lateral directions with Indices 1, 2, and 3 accordingly, we can write the average principal stretches in the form

$$\lambda_1 = \frac{dr}{dR}, \quad \lambda_2 = \frac{r}{R}, \quad \lambda_3 = \frac{h}{H}. \tag{25}$$

The constitutive equations relate the average stretches to the components of the 1st Piola–Kirchhoff stress tensor, $\mathbf{P}$, as follows

$$\begin{aligned} P_1 &= P_{rR} = \frac{\partial \psi}{\partial \lambda_1} - p\lambda_1^{-1} \\ P_2 &= P_{\vartheta\Theta} = \frac{\partial \psi}{\partial \lambda_2} - p\lambda_2^{-1} \\ P_3 &= P_{zZ} = \frac{\partial \psi}{\partial \lambda_3} - p\lambda_3^{-1} \end{aligned} \tag{26}$$

where p is the indefinite Lagrange multiplier enforcing the incompressibility condition

$$\lambda_1\lambda_2\lambda_3 = 1. \tag{27}$$

Since the membrane faces are stress-free, $P_{zZ} = 0$, we can exclude the Lagrange multiplier from (26)

$$\begin{aligned} P_1 = \ P_{rR} &= \frac{\partial \psi}{\partial \lambda_1} - \frac{\lambda_3}{\lambda_1}\frac{\partial \psi}{\partial \lambda_3} \\ P_2 = P_{\vartheta\Theta} &= \frac{\partial \psi}{\partial \lambda_2} - \frac{\lambda_3}{\lambda_2}\frac{\partial \psi}{\partial \lambda_3}. \end{aligned} \tag{28}$$

It is worth reminding again that the principal values of the 1st Piola–Kirchhoff stress tensor correspond to the thickness average stretches.

Now, the equilibrium equations with respect to referential coordinates [Volokh, 2006] will reduce to

$$\frac{dP_1}{dR} + \frac{P_1 - P_2}{R} = 0. \tag{29}$$

This equation is completed by the conditions at the membrane edges

$$P_1(A) = 0, \quad P_1(B)\lambda_1(B) = g, \tag{30}$$

where g is the value of the hydrostatic tension.

Normalizing the length scale by the radius of the initial cavity we introduce

$$\lambda_1 = \frac{d\bar{r}}{d\bar{R}} = \frac{dr}{dR}, \quad \lambda_2 = \frac{\bar{r}}{\bar{R}} = \frac{r}{R}, \quad \lambda_3 = \frac{\bar{h}}{\bar{H}} = \frac{h}{H}, \tag{31}$$

$$\bar{r} = \frac{r}{A}, \quad \bar{R} = \frac{R}{A}, \quad \bar{h} = \frac{h}{A}, \quad \bar{H} = \frac{H}{A}, \quad \bar{A} = 1, \quad \bar{B} = \frac{B}{A}. \tag{32}$$

Substituting (31)–(32) in (29)–(30) we obtain the two-point boundary value problem

$$\frac{dP_1}{d\bar{R}} + \frac{P_1 - P_2}{\bar{R}} = 0, \tag{33}$$

$$P_1(1) = 0, \quad P_1(\bar{B})\lambda_1(\bar{B}) = g, \tag{34}$$

where the principal stresses are defined in (28) and principal stretches are defined in (31) with account of the incompressibility condition (27).

Equation (33) and boundary conditions (34) can be solved numerically for $\bar{r}(\bar{R})$ with account of (27), (28), and (31). In the case of $\bar{B} \gg 1$ we have the problem of the expansion of small void in the infinite membrane under the biaxial tension.[4]

Since our purpose is to track the stress-stretch curve, there is no need to solve the two-point boundary value problem for the given hydrostatic tension, g. Instead, it is reasonable to solve a simpler initial value problem defined by the following conditions at point $\bar{A} = 1$:

$$\bar{r}(1) = a/A, \quad \frac{d\bar{r}}{d\bar{R}}(1) = \beta. \tag{35}$$

Here β is defined from $(34)_1$ by solving the algebraic equation

$$\frac{\partial \psi}{\partial \lambda_1} - \frac{\lambda_3}{\lambda_1}\frac{\partial \psi}{\partial \lambda_3} = 0, \tag{36}$$

where

$$\lambda_1 = \beta, \quad \lambda_2 = \frac{a}{A}, \quad \lambda_3 = \frac{1}{\lambda_1 \lambda_2}. \tag{37}$$

By the direct calculation we obtain

$$\frac{\partial \psi}{\partial \lambda_1} = \frac{\partial \psi}{\partial W}\frac{\partial W}{\partial \lambda_1} = \frac{\partial \psi}{\partial W} 2\lambda_1 \sum_{k=1}^{3} kC_{k0}(\lambda_1^2 + \lambda_2^2 + \lambda_3^2 - 3)^{k-1}, \tag{38}$$

$$\frac{\partial \psi}{\partial \lambda_3} = \frac{\partial \psi}{\partial W}\frac{\partial W}{\partial \lambda_3} = \frac{\partial \psi}{\partial W} 2\lambda_3 \sum_{k=1}^{3} kC_{k0}(\lambda_1^2 + \lambda_2^2 + \lambda_3^2 - 3)^{k-1}. \tag{39}$$

Substituting (38)–(39) in (36) we get

$$\lambda_1^2 = \lambda_3^2. \tag{40}$$

Finally, substituting (37) in (40) we have

$$\beta = \sqrt{\frac{A}{a}}. \tag{41}$$

Now the solution of (33) and (35) can be generated numerically for varying a and g is the outcome of the calculation, as shown in Figs. 7 and 8.

[4]In computations we have assumed: $\bar{B} = 1000$.

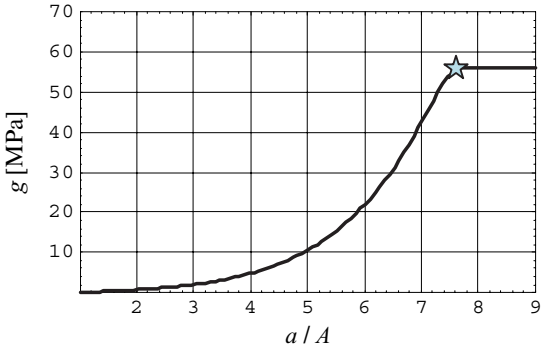

Fig. 7. Membrane void: hydrostatic tension versus void hoop stretch for NR.

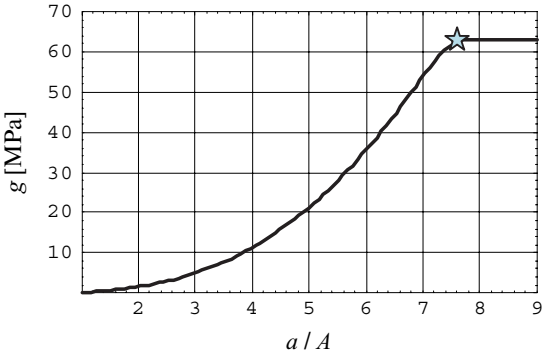

Fig. 8. Membrane void: hydrostatic tension versus void hoop stretch for SBR.

The results show that starting from the tension of 56 MPa for natural rubber and 63 MPa for styrene-butadiene rubber, the void starts expanding in the unstable mode. Parallel to the results of the previous section, the instability point corresponds to the similar critical hoop stretch for both materials at the void edge: $a/A = 7.5$.

5. Discussion

The problem of the void expansion in rubberlike materials was addressed by many authors who used various approaches. In the present work, we also addressed this problem using a new approach of the elasticity with energy limiters, which allowed enforcing a material failure description in the constitutive equations. Specifically, we used the failure enhanced models of natural and styrene-butadiene rubbers calibrated in experiments to calculate the critical hydrostatic tension imposed remotely on bulk and membrane voids. For NR and SBR we found that the critical magnitude of the bulk hydrostatic tension is about $2 \div 3$ MPa and the membrane tension is about $50 \div 60$ MPa. These magnitudes of the hydrostatic and membrane tension correspond to the critical void hoop stretches equal 5.4 and 7.5 accordingly. It should

not be missed, of course, that though the critical value of the hydrostatic tension is smaller than the critical value of the membrane tension the critical *integral* force that is imposed on the bulk void is proportional to the surface area of a 3D sphere while the critical *integral* force that is imposed on the membrane void is proportional to the perimeter of a 2D circle times the membrane thickness. Consequently, the integral force on the void in the bulk will be generally greater than the integral force on the membrane void.

It is hoped that the obtained critical parameters of the void instability will be helpful in the design structural elements made of rubber.

References

Abeyaratne, R. and Horgan, C. O. [1985] "Initiation of localized plane deformations at a circular cavity in an infinite compressible nonlinearly elastic medium," *J. Elasticity* **15**, 243–256.

Ball, J. M. [1982] "Discontinuous equilibrium solutions and cavitation in nonlinear elasticity. Phil. Trans. Royal Soc. London. Series A," *Math. Phys. Eng. Sciences* **306**, 557–611.

Bassani, J. L., Durban, D. and Hutchinson, J. W. [1980] "Bifurcation of a spherical hole in an infinite elastoplastic medium," *Math. Proc. Cambridge Phil. Society* **87**, 339–356.

Beatty, M. F. [1987] "Topics in finite elasticity: Hyperelasticity of rubber, elastomers and biological tissues — with examples," *Appl. Mech. Rev.* **40**, 1699–1734.

Cohen, T. and Durban, D. [2010] "Cavitation in elastic and hyperelastic sheets," *Int. J. Engrg. Sci.* **48**, 52–66.

Durban, D. and Baruch, M. [1976] "On the problem of a spherical cavity in an infinite elasto-plastic medium," *J. Appl. Mech.* **43**, 633–638.

Durban, D. and Birman, V. [1982] "On the elasto-plastic stress concentration at a circular hole in an anisotropic sheet," *Acta Mech.* **43**, 73–84.

Fond, C. [2001] "Cavitation criterion for rubber materials: A review of void-growth models," *J. Polymer Sci.: Part B: Polymer Phys.* **39**, 2081–2096.

Gent, A. N. [1990] "Cavitation in rubber: A cautionary tale," *Rub. Chem. Technol.* **63**, G49–G53.

Hamdi, A., Nait Abdelaziz, M., Ait Hocine, N., Heuillet, P. and Benseddiq, N. [2006] "A fracture criterion of rubber-like materials under plane stress conditions," *Polymer Testing* **25**, 994–1005.

Haughton, D. M. [1986] "On non-existence of cavitation in incompressible elastic membranes," *Q. J. Mech. Appl. Math.* **39**, 289–296.

Haughton, D. M. [1990] "Cavitation in compressible elastic membranes," *Int. J. Engrg. Sci.* **28**, 163–168.

Henao, D. [2009] "Cavitation, invertibility, and convergence of regularized minimizers in nonlinear elasticity," *J. Elasticity* **94**, 55–68.

Horgan, C. O. and Polignone, D. A. [1995] "Cavitation in nonlinearly elastic solids: A review," *Appl. Mech. Rev.* **48**, 471–485.

Hou, H.-S. and Abeyaratne, R. [1992] "Cavitation in elastic and elastic-plastic solids," *J. Mech. Phys. Solids* **40**, 571–592.

Huang, Y., Hutchinson, J. W. and Tvergaard, V. [1991] "Cavitation instabilities in elastic-plastic solids," *J. Mech. Phys. Solids* **39**, 223–241.

Lopez-Pamies, O. [2009] "Onset of cavitation in compressible, isotropic, hyperelastic solids," *J. Elasticity* **94**, 115–145.

Ogden, R. W. [2003] "Nonlinear elasticity, anisotropy, material stability and residual stresses in soft tissue, in *Biomechanics of Soft Tissue in Cardiovascular systems*, eds. Holzapfel, G. A. and Ogden, R. W. Vienna, Austria: Springer, *CISM Courses and Lectures*, **441**, pp. 65–108.

Trapper, P. and Volokh, K. Y. [2010] "Modeling dynamic failure in rubber," *Int. J. Fracture* **162**, 245–253.

Volokh, K. Y. [2006] "Lagrangian equilibrium equations in cylindrical and spherical coordinates," *Comp. Mat. Continua* **3**, 37–42.

Volokh, K. Y. [2007] "Hyperelasticity with softening for modeling materials failure," *J. Mech. Phys. Solids* **55**, 2237–2264.

Volokh, K. Y. [2008] "Multiscale modeling of material failure: From atomic bonds to elasticity with energy limiters," *J. Multiscale Comp. Engrg.* **6**, 393–410.

Volokh, K. Y. [2010] "On modeling failure of rubber-like materials," *Mech. Res. Com.* **37**, 684–689.

Volokh, K. Y. [2011] "Characteristic length of damage localization in rubber," *Int. J. Fracture* **168**, 113–116.

Volokh, K. Y. and Vorp, D. A. [2008] "A model of growth and rupture of abdominal aortic aneurysm," *J. Biomech.* **41**, 1015–1021.

Williams, M. L. and Schapery, R. A. [1965] "Spherical flow instability in hydrostatic tension," *Int. J. Fracture* **1**, 64–72.

Xinchun, S. and Changjun, C. [2002] "Cavitation in Hookean elastic membranes," *Acta Mech. Solid Sinica* **15**, 89–94.